Connectedness percolation of fractal liquids

Please check the document version of this publication:

Connectedness percolation of fractal liquids

René de Bruijn [1,2,*] and Paul van der Schoot [1]

[1]*Department of Applied Physics, Eindhoven University of Technology, P.O. Box 513, 5600 MB Eindhoven, The Netherlands*
[2]*Institute for Complex Molecular Systems, Eindhoven University of Technology, P.O. Box 513, 5600 MB Eindhoven, The Netherlands*

We apply connectedness percolation theory to fractal liquids of hard particles, and make use of a Percus-Yevick liquid state theory combined with a geometric connectivity criterion. We find that in fractal dimensions the percolation threshold interpolates continuously between integer-dimensional values, and that it decreases monotonically with increasing (fractal) dimension. The influence of hard-core interactions is significant only for dimensions below three. Finally, our theory incorrectly suggests that a percolation threshold is absent below about two dimensions, which we attribute to the breakdown of the connectedness Percus-Yevick closure.

I. INTRODUCTION

Recently, Heinen *et al.* introduced *fractal liquids* in which both the particles and the embedding space are treated as objects of the same fractal dimension [1]. Such liquids are therefore fractal at all length scales. This contrasts with the more familiar case of fluids confined in porous media, which are often thought to represent a fractal geometry. In liquid-state theory, the *local* structure of the confining medium is in that case usually modeled as a sphere, cylinder, or slit [2,3], and any connection to the fractal background lost. Exceptions are so-called quenched-annealed liquids of which the constituent model particles share the volume with confining obstacles the distribution of which is fixed in space [4–6].

Confinement is known to have a significant impact on thermal phase transitions, e.g., by shifting the critical point, changing the order of the phase transition, or even causing a phase transition to be absent altogether [7–12]. This is mirrored, on the one hand, in theoretical studies of phase transitions in cylinders [13–15] and slits [12,14–16], and, on the other hand, by those that *effectively* describe the actual structure of a porous medium. In the latter, the fractal geometry is either inscribed explicitly in a lattice [17,18] or treated implicitly by a random disorder field in continuum field theories [19–22].

In the theory of fractal liquids, however, the porosity of the confining medium is described by a single (fractal) dimension, so without any reference to a Euclidean embedding space, and specific interactions with the confining walls are ignored [1]. The predictions of Heinen *et al.* for the microscopic fluid structure, obtained using a generalized Percus-Yevick approach, agree very well with results from their Monte Carlo simulations [1]. Actual realizations of this model may perhaps be found in binary microphase-separated liquids in porous media if the characteristic size of the (macroscopic) liquid droplets is very much larger than the porosity length scale.

As far as we are aware, phase transitions in fractal liquids have not yet been investigated. Hence, in this article, we focus attention on the geometric percolation transition in fractal liquids, which belongs to a particular class of (second-order) phase transition [23]. The percolation phase transition describes the transition from a locally to a globally connected network of particles and so involves a diverging cluster size. It differs from the aforementioned thermal phase transitions by the introduction of an additional "connectedness" parameter that describe particle-particle connections [24]. This parameter does not influence the equilibrium thermodynamic properties of the material itself and is often modeled by a simple distance criterion. It is, however, an intrinsic property of a physical system and its actual value relies on, e.g., the properties of the host medium and the mode of transport. In the case of electrical tunneling percolation, it is related to the effective tunneling length of charge carriers [25,26].

We are particularly interested in the influence of the fractal dimension D on the percolation threshold, defined as the filler fraction at which a material-spanning cluster emerges, and the critical exponent γ, associated with the mean cluster size. To calculate these quantities, we make use of the Percus-Yevick integral equation theory for fractal liquids of Heinen and collaborators [1] and apply it to geometrical percolation where connectivity is defined by a distance criterion. In our so-called cherry-pit model, the particles have an impenetrable core of diameter σ and direct connections are identified by this distance criterion λ. In principle, both the percolation threshold and the critical exponent γ depend on the ratio σ/λ. As far as we are aware, connectedness Percus-Yevick theory within the cherry-pit model has been analyzed only in $D = 3$ [27], and our analysis extends to both integer and noninteger dimensions between one and six.

Both the thermal Percus-Yevick (PY) and the connectedness Percus-Yevick (cPY) theory are approximate integral equation theories based on the exact Ornstein-Zernike formalism [24,28]. PY theory is commonly used to predict the equilibrium structure and correlations in simple liquids of particle characterized by strongly repulsive interactions, where

_____
*r.a.j.d.bruijn@tue.nl

it is well known to be very accurate at low to intermediate densities [28]. At high densities, however, this is less so as it does not predict a liquid-solid transition and can even yield unphysical results, such as a locally negatively valued pair correlation function [28,29]. Interestingly, it turns out to be an exact theory for hard rods in one dimension [30]. cPY theory is derived from PY theory and so is based on the same set of approximations, and is known to be less accurate in predicting percolation properties than PY theory is in predicting thermodynamic properties. This is caused by fortuitous cancellation of errors occurring to a lesser extend in cPY theory compared to PY theory [27,31].

According to our findings, the geometric percolation threshold of fractal liquids of hard particles interpolates in a continuous manner between those of integer-dimensional fluids of isometric particles, and decreases monotonically with increasing fractal dimension. The critical exponent γ also decreases with increasing dimensionality and approaches the mean-field value of unity already in five dimensions. This is below the accepted upper critical dimension of six [23]. Surprisingly, our calculations indicate that connectedness PY theory breaks down approaching two dimensions from above: the critical exponent γ diverges for $D \downarrow 2$, and in that case we fail to find a system-spanning cluster at finite densities. Interestingly, we find that the value of σ/λ either weakly impacts upon our findings or not at all.

The remainder of this paper is structured as follows. In Sec. II we introduce the theory of fractal liquids, and we generalize connectedness percolation theory accordingly. In Sec. III we present our results on the percolation threshold and the mean cluster size critical exponent. We discuss the effects of the fractal dimension and the hard core fraction σ/λ on both the percolation threshold and the critical exponent. Finally, we present our conclusions in Sec. IV.

II. THEORY AND METHODS

Before going into the details of our calculations, we first introduce two concepts that are relevant in the context of the fractal nature of our particles and the space they live in. The first point we need to address is that the relevant distance measure is *not* the Euclidean but the so-called *chemical* distance, where the distance between two points is measured along the fractal embedding space [1]. In lattice terminology, this translates to the shortest connected path between two sites [1]. Further, the relevant (fractal) dimension in the model identified by Heinen and co-workers is the *spreading dimension* d_l. It is related to the chemical distance by the scaling of the number of sites (or "mass") $\mathcal{N}$ that are within the chemical distance l_{chem} from any site via $\mathcal{N} \sim l_{\text{chem}}^{d_l}$ [1]. In integer dimensions, where the chemical distance coincides with the Euclidean distance, the spreading dimension coincides with the spatial dimension.

With these definitions, we can now generalize our cherry-pit particle model to fractal dimensions. In lattice terminology, we define the fractal dimensional equivalent of a hard core particle with "diameter" σ, as all nodes that lie within a chemical distance of $\sigma/2$ removed from the center node. Moreover, the fractal particles have a connectivity shell of diameter λ around this hard core. If the chemical distance between the

centers of two particles is less than λ, yet larger than σ, we define the particles to be connected. Due to the hard core repulsion, the centers of two particles cannot be within a chemical distance of σ.

Our theoretical description of geometric percolation is based on connectedness Ornstein-Zernike (cOZ) theory [24]. Within this formalism, the cluster size is given by $S = 1 + \rho \lim_{q \to 0} \widehat{P}(q)$, where ρ is the number density and $\widehat{P}(q)$ is the Fourier transform of the so-called pair connectedness function $P(r)$. The pair connectedness function describes the probability that two particles, separated by a center-to-center distance $r = |\mathbf{r}|$, are connected. It is connected to the function $C^+(r)$ known as the direct connectedness function, via the cOZ equation $P(r) = C^+(r) + \rho \int d^D \mathbf{r}' P(r') C^+(|\mathbf{r} - \mathbf{r}'|)$, with D again the spreading dimension, $C^+(r)$ encoding the specific subset of connections between pairs of particle that remain connected upon removal of any other particle connected to these two [24].

Obviously, since $C^+(r)$ is unknown *a priori*, the cOZ equation needs to be supplemented by a closure relation. We employ the connectedness PY or cPY closure, defined by the conditions $P(r \leqslant \lambda) = g(r)$, and $C^+(r > \lambda) = 0$ [27]. The latter imposes the presumed short-distance nature of the direct connectedness function. That the former is sensible follows from the fact that the radial distribution function $g(r)$ describes the probability to find a particle at r around a test particle that is placed at the origin. Our motivation for using the cPY closure is that it is relatively straightforwardly generalized to fractal liquids, devoid of any adjustable parameters, and because analytical results are known for certain cases, we can directly evaluate the accuracy of our methods [32].

The radial distribution function itself can be obtained from the liquid-state Ornstein-Zernike (OZ) equation $g(r) = 1 + c(r) + \rho \int d^D \mathbf{r}'[g(|\mathbf{r}'|) - 1]c(|\mathbf{r} - \mathbf{r}'|)$, which also needs to be closed. As we use the Percus-Yevick closure for the cOZ equation we invoke the same closure here, implying that for hard particles we insist on the no-overlap condition $g(r \leqslant \sigma) = 0$ and set $c(r > \sigma) = 0$ [28]. We note that for ideal particles $g(r) = 1$ for all $r \geqslant 0$, and only the cOZ equation needs to be solved, which we do numerically, simplifying our calculations considerably. For cherry-pit particles with $\sigma/\lambda > 0$, we numerically solve the OZ and cOZ equations consecutively, and rely on the same method used by Heinen and co-workers, that is, by exploiting a generalized Hankel transform that can be dimensionally continued (see Appendix A) [1].

Finally, we pinpoint the particle density at the percolation threshold ρ_p, or in dimensionless form η_p, by the condition $S \to \infty$. This we also do numerically, making use of the scaling relation for the mean cluster size $S \propto |\eta - \eta_p|^{-\gamma}$ presumed to be valid for $\eta \to \eta_p$. Here, γ is the appropriate critical exponent. The quantities η_p and γ we asymptotically fit in the critical region of the mean cluster size S. We have tested this procedure and compare it against the exact analytical results for ideal particles in $D = 3$ and 5, and find the error in the percolation threshold η_p to be negligible (less than $10^{-2}\%$). The error in the critical exponent γ is somewhat larger, up to 4% from the analytically obtained values. See Appendix A for a detailed discussion.
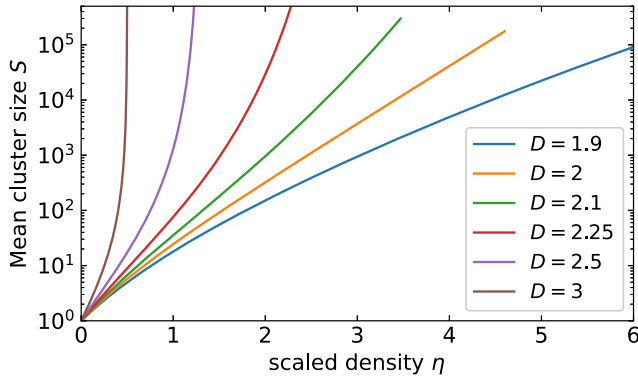
FIG. 1. The mean cluster size $S(D)$ obtained within cPY theory as function of the scaled density η, defined as the number density scaled with the volume of a D-dimensional sphere of diameter λ.

III. RESULTS AND DISCUSSION

Starting with our results for ideal, noninteractig fractal particles ($\sigma/\lambda = 0$), Fig. 1 shows how according to our calculations the mean cluster size $S(D)$ depends on the scaled density $\eta \equiv 2\pi^{D/2}(\lambda/2)^D\rho/D\Gamma(D/2)$, for selected dimensionalities D between 1.9 and 3.0. Here, ρ is the number density of the ideal particles of "diameter" λ, and $2\pi^{D/2}(\lambda/2)^D/D\Gamma(D/2)$ the volume of a D-dimensional sphere with diameter λ. As the percolation threshold is the scaled density for which the mean cluster size S diverges, we deduce from Fig. 1 that within cPY theory this seems not to occur for $D \leqslant 2$.

For $D = 2$, the mean cluster size grows exponentially up to the largest density of 4.6 that in our calculations produce a convergent cluster size. This, incorrectly, suggests that for $D = 2$ it formally diverges at an infinite density. In this context, it is useful to note that this should certainly happen for $D = 1$. Indeed, the exact result for the cluster size in *one* dimension reads $S(1) = 2\exp\eta - 1$. If we compare this with the prediction of cPY theory, $S_{\mathrm{PY}}(1) = (1 + \eta)^2$, then it transpires that both remain finite at finite density but differ considerably in functional form [33]. This calls into question the validity of cPY theory for $D \leqslant 2$.

The obvious question that now arises is how well cPY fares for $D > 2$. Fig. 1 suggests that for $D > 2$ the mean cluster size diverges at a finite density. Indeed, the analytical solution of cPY theory for $\sigma/\lambda = 0$ in the *integer* dimension $D = 3$ gives a percolation threshold of $\eta = \eta_{\mathrm{p}} = 1/2$. For $D = 5$, we find $\eta = 3/2 - 5/6\sqrt{3}$. The former overestimates Monte Carlo simulation results [34] by almost 50%, while the latter overestimates Monte Carlo results by about 4% [35]. In Fig. 2 we show our numerically obtained percolation threshold for the cases $\sigma/\lambda = 0$ and 0.5 as function of the (fractal) dimension D, and compare these with simulation results for integer dimensions $D = 2 - 6$. It shows that the presence of a hard core does not appreciably affect the percolation threshold.

For $D < 3$, the percolation threshold increases sharply with decreasing dimension, and appears to diverge upon approach of $D \downarrow 2$, although we have not been able to extract the percolation threshold for $D < 2.25$. This supports our previous assessment based on Fig. 1. For integer $D \geqslant 4$, theory and
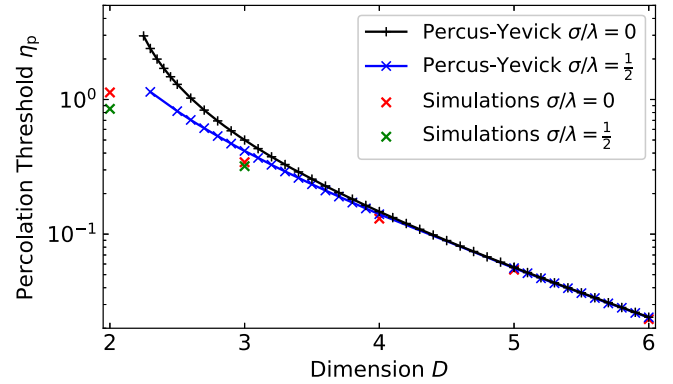

FIG. 2. The percolation threshold η_{p} as function of the spatial dimension D for cherry-pit particles with $\sigma/\lambda = 0$ (black, plus signs) and $\sigma/\lambda = 1/2$ (blue, crosses). The percolation threshold is expressed as the number density scaled with the volume of a D-dimensional sphere of diameter λ. Results obtained from Monte Carlo simulations for $\sigma/\lambda = 0$ (red) are taken from Ref. [35], and for $\sigma/\lambda = 1/2$ from Ref. [39,40] (green).

simulations agree almost quantitatively, with the percolation threshold decreasing with increasing dimension. A decreasing η_{p} with increasing D is to be expected if we take the percolation threshold to be inversely proportional to the volume available for two particles to remain connected [35–37]. To leading order this gives $\eta_{\mathrm{p}} \propto 2^{-D}$, which becomes exact in infinite dimensions [37,38].

Having discussed our results for the percolation threshold for ideal particles, we now extend our treatment to cherry-pit particles. These results are summarized in Fig. 3. Shown in Fig. 3(a) is the percolation threshold as function of the hard-core fraction σ/λ for selected dimensions, and we highlight the influence of the hard-core fraction on the percolation threshold in Fig. 3(b), where we have scaled the percolation threshold η_{p} to its value for $\sigma/\lambda = 0$.

We restrict ourselves to those results for which we can pinpoint the percolation threshold accurately, that is, for $D > 2.25$. We notice that, starting at $\sigma/\lambda = 0$, the percolation threshold decreases with increasing σ/λ albeit that the effect is larger the smaller the dimensionality of space, which is especially transparent in Fig. 3(b). However, for $D \geqslant 2.5$, we find that the percolation threshold increases again, i.e., there is a well-defined minimum for some value of $\sigma/\lambda > 0$ that depends on the value of D.

For $D = 2$ and 3, this nonmonotonic behavior can be explained in terms of two counteracting many-body effects [41]. The first is connected with that fewer particles are, on average, required to span a certain distance in the presence of a hard core, and moreover these configurations are more probable due to local crowding of particles around that hard core. This effect *decreases* the percolation threshold. The second effect is caused by the connectivity shell becoming smaller with increasing value of σ/λ. The concomitant decrease in contact volume *increases* the percolation threshold. The former effect predominates more strongly in lower dimensional spaces, because the available "volume" per particle decreases with decreasing dimensionality.
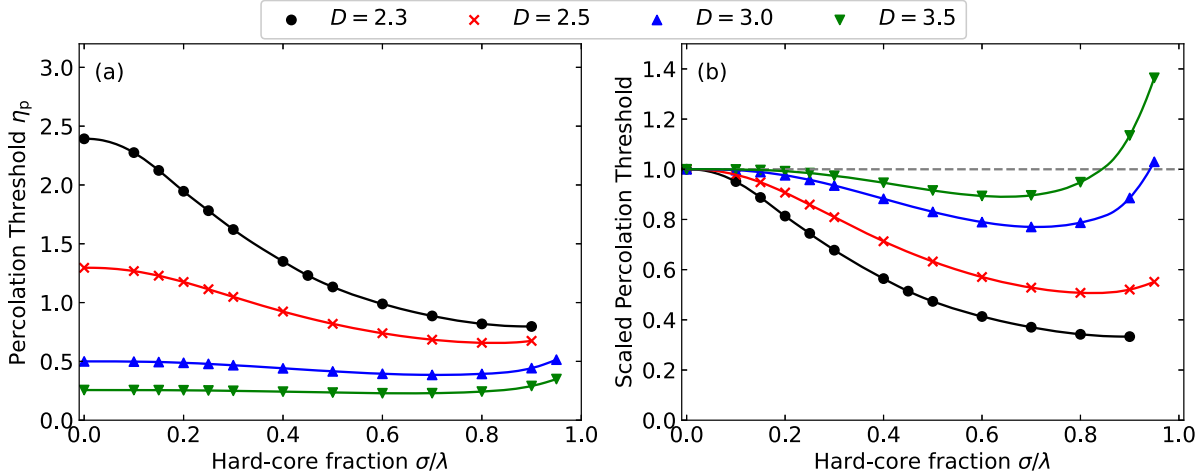
FIG. 3. Left: The percolation threshold η_p, expressed as the number density scaled with the volume of a D-dimensional sphere of diameter λ, as function of the hard core fraction σ/λ for spatial dimensions $D = 2.3$ (dots), 2.5 (crosses), 3.0 (triangle up), and 3.5 (triangle down). Here, σ is the hard core diameter, and λ the diameter of the connectivity shell. The lines are a spline fit through the data as a guide for the eye. Right: The same data with the percolation threshold scaled via $\eta_p(\sigma/\lambda)/\eta_p(\sigma/\lambda = 0)$. The lines are a spline fit through the data as a guide for the eye.

Of the findings presented in Fig. 3, only those for $D = 3$ allow for comparison with Monte Carlo simulations reported on in the literature [40]. As is well known, cPY predictions deviate by approximately 46% for $\sigma/\lambda = 0$, but the difference decreases with increasing σ/λ down to 14% for $\sigma/\lambda = 0.95$. Incidentally, for $\sigma/\lambda > 0.95$ percolation is preempted then by a transition to a crystal phase [27,40]. If we stay below the crystal transition, we expect cPY to be most accurate for small connectivity ranges for all $D > 1$, not just $D = 3$. The reason is that with increasing σ/λ, the cluster structure becomes increasingly more tree-like [42]. Nevertheless, the observation from Fig. 2 that the theory becomes less accurate for $D < 3$ generalizes for all $0 \leqslant \sigma/\lambda \leqslant 1$.

Taking cPY at face value for all D and σ/λ, then both Fig. 2 and Fig. 3 lead us to the conclusion that the percolation threshold must rise substantially upon approaching two dimensions from above. Associated with this apparent divergence in the percolation threshold, we find a divergence of the critical exponent γ. Our most accurate estimate for γ we obtain for the case $\sigma/\lambda = 0$ and is presented in Fig. 4. We do not expect that a nonzero σ/λ changes this as the cherry-pit and ideal models should be in the same universality class [27,31]. Representative findings for $\sigma/\lambda > 0$, presented in Appendix B, support this.

As is evident from Fig. 4, the critical exponent interpolates continuously between the known cPY exponent in three dimensions $\gamma = 2$ and the exponent $\gamma = 1$ obtained by us for $D = 5$ (see Appendix C). It shows the same trend as the results from Monte Carlo simulations, also indicated, where γ increases with decreasing value of D. We note that the critical exponent we find for $D = 5$ is the mean-field value, yet the generally accepted upper critical dimension for both lattice and continuum percolation is $D = 6$ [23].

The sharp rise of the critical exponent when the dimensionality of space drops below three contrasts with the simulation results. In the inset of Fig. 4 we suggest that γ scales as $\gamma = 2/(D - 2)$ for $2 < D < 3$, which indeed points at γ diverging

for $D \to 2$. Incidentally, a similar divergence is known to occur in the spherical model of ferromagnetism [43]. This strengthens our conclusion that cPY theory breaks down near $D = 2$.

It is not clear exactly why cPY theory fails near two dimensions. Of course, we cannot exclude the possibility that it is not cPY theory itself that lies at the root of the problem but some numerical issue. Still, it should not come as a complete surprise, because percolation is essentially a high-density phenomenon as Fig. 2 also shows. For *penetrable* particles, the actual fraction of the volume covered by particles at the percolation threshold is $\phi_p = 1 - \exp(-\eta_p) \approx 0.67$ in two dimensions compared to $\phi_p \approx 0.28$ in three dimensions and to $\phi_p \approx 0.12$ in four [23]. It follows that the long-ranged loop
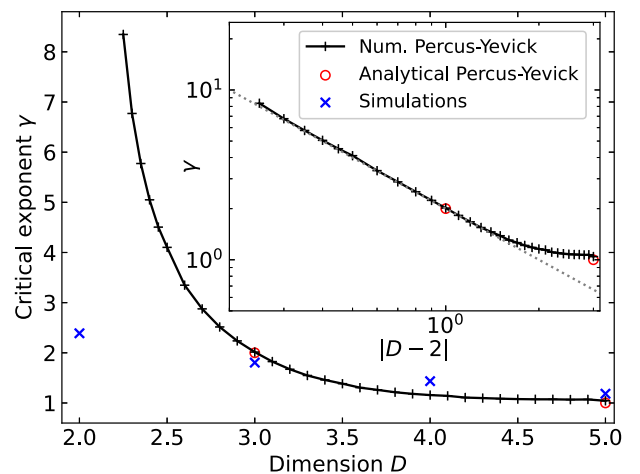

FIG. 4. Main: The critical exponent γ within cPY theory both numerically (black, plus signs) and theoretically (red, circles), and from simulations (blue, crosses) [27,44]. Inset: The critical exponent γ as function of the shifted dimension $|D - 2|$, where including the scaling $\gamma \sim 2/(D - 2)$ (grey, dotted).

connections that cPY theory neglects must become increasingly important when lowering the dimensionality of space [45]. There is no reason to suspect this not also to be true for hard particles [39]. As is becoming increasingly clear, closures that are accurate in the context of thermodynamic liquid-state theory are not necessarily accurate in the context of percolation, in particular in low-dimensional systems [46], and that they have to be adapted for that purpose [45].

IV. CONCLUSIONS

In conclusion, we have investigated the geometrical percolation transition in fractal liquids within a cherry-pit model and applied for that the Percus-Yevick approximation. We find that the continuum percolation threshold in noninteger dimensions interpolates continuously between the integer-dimensional values, and decreases with increasing dimension. The same conclusion holds for the critical exponent γ, which within Percus-Yevick theory attains its mean-field value in five dimensions, below the generally accepted upper critical dimension of six. Interestingly, hard-core interactions affect the percolation threshold only marginally, in particular in higher-dimensional spaces. Below three dimensions, the percolation threshold η_p as well as the critical exponent γ diverge as $D \to 2$. This contrasts with the known finite percolation threshold and critical exponent for $D = 2$, and signifies the breakdown of connectedness Percus-Yevick theory below three dimensions.

APPENDIX A: NUMERICAL SOLUTION STRATEGY

We determine the onset of a material-spanning cluster, i.e., the percolation threshold, as the number density ρ where the mean cluster size

$$S = 1 + \rho \lim_{q \to 0} \widehat{P}(q) \tag{A1}$$

diverges. Here, $\widehat{P}(q)$ is the Fourier transform of the pair connectedness function with $q = |\mathbf{q}|$ the magnitude of the momentum transfer vector. The pair connectedness function we obtain from the connectedness Ornstein-Zernike (cOZ) equation

$$P(r) = C^+(r) + \rho \int d^D\mathbf{r}'P(r')C^+(|\mathbf{r} - \mathbf{r}'|), \tag{A2}$$

where $r = |\mathbf{r}|$ is the magnitude of the separation vector, $C^+(r)$ the direct connectedness function, ρ the number density, and D the (spreading) dimension. For nonideal particles, we additionally require the liquid-state Ornstein-Zernike (OZ) equation in order to obtain the radial distribution function $g(r)$

$$g(r) = 1 + c(r) + \rho \int d^D\mathbf{r}'[g(|\mathbf{r}|) - 1]c(|\mathbf{r} - \mathbf{r}'|), \tag{A3}$$

where $c(r)$ the direct correlation function. For isotropic systems these equations reduce to algebraic equations in Fourier space

$$\widehat{P}(q) = \frac{\widehat{C}^+(q)}{1 - \rho\widehat{C}^+(q)} \tag{A4}$$

and

$$\widehat{g}(q) = \frac{1 + \widehat{c}(q)}{1 - \rho\widehat{c}(q)}, \tag{A5}$$

with $q = |\mathbf{q}|$ the magnitude of the momentum transfer vector.

Since the (connectedness) Percus-Yevick closure is implemented in real space, our (iterative) numerical solution strategy employs a spectral solver, which is based on the generalized D-dimensional Hankel transform pair

$$\widehat{f}(q) = \frac{(2\pi)^{D/2}}{q^{D/2-1}} \int_0^\infty dr\, r^{D/2} J_{D/2-1}(qr)f(r), \tag{A6}$$

$$f(r) = \frac{r^{1-D/2}}{(2\pi)^{D/2}} \int_0^\infty dq\, q^{D/2} J_{D/2-1}(qr)\widehat{f}(q), \tag{A7}$$

valid for a D-dimensional isotropic function $f(r)$. Here, $J_{D/2-1}(x)$ is the Bessel function of the first kind and order $D/2 - 1$, which is analytic with respect to both $D \geqslant 1$ and $q, r > 0$. The Hankel transforms are calculated using a sampling technique based on a logarithmic grid [1,47–49], which is equivalent to the approach by Heinen and co-workers [1].

We numerically solve the set of equations by a modified Picard iteration, where we improve the stability of our numerical solver using the modified direct inversion of iterative subspace (MDIIS) approach [50]. To find the percolation threshold, we initiate our solver for a given dimension D at a sufficiently low density. Next, we incrementally increase the density, solving the equations at every increment until we reach a density where the solver does not converge to a solution within 200 iterations. It turns out that this density does not necessarily coincide with the percolation threshold, and is therefore associated with limited convergence of our numerical solver at high densities and close to the percolation threshold. In spite of, we can still accurately extrapolate the percolation threshold and determine the critical exponent of the mean cluster size by fitting our numerical solution for the mean cluster size to the scaling law

$$S \sim |\eta - \eta_p|^{-\gamma}, \tag{A8}$$

with γ a critical exponent, η the scaled density, defined as the number density scaled with the volume of a D-dimensional sphere of diameter λ, and η_p the percolation threshold.

The accuracy of our numerical solutions we validate by comparing our predictions with known analytical solutions of the connectedness Percus-Yevick equations. Figure 5 shows the relative error between our numerically obtained mean cluster size S, and the known analytical results for $D = 1$, $D = 3$, and $D = 5$ for $\sigma/\lambda = 0$. Clearly, away from the percolation threshold the error is negligible. Only near the percolation threshold the errors increase sharply. This we associate to the pair connectedness function $P(r)$ becoming long-ranged near the percolation threshold. We further note that we have also compared our numerical results for $D = 3$ and $1/2 < \sigma/\lambda < 1$ to the known analytical values, and find the agreement to be similar as the $D = 3$, $\sigma/\lambda = 0$ case shown in Fig. 5 (data not shown).
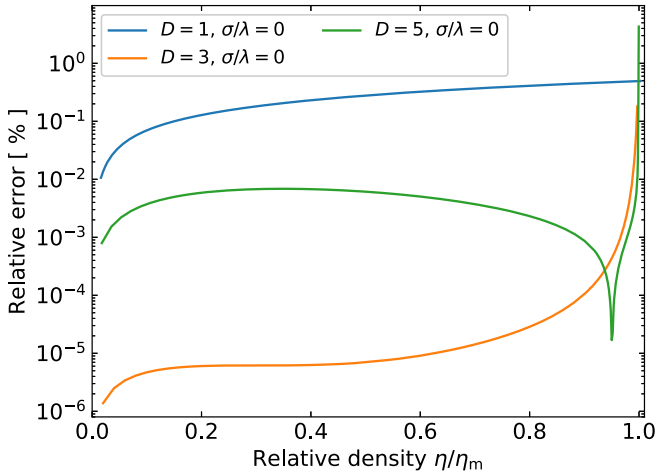
FIG. 5. The error in our numerically obtained mean cluster size S and the known analytic solution to cPY theory, as a function of the scaled density η/η_m, where for $D = 1$, η_m is the highest density our solver converges ($\eta_m = 25$), and for $D = 3$ and $D = 5$ η_m is the percolation threshold $\eta_m = \eta_p = 1/2$ and $\eta_m = \eta_p = 3/2 - 5/6\sqrt{3}$, respectively.

The aforementioned extrapolation procedure based on the scaling relation is particularly relevant in low dimensional spaces, where we find that distance between the percolation threshold and the density up to which our solver converges increases with decreasing dimension, as shown in Fig. 6. Our extrapolation scheme works well only if we can approach the percolation threshold sufficiently close. This appears to not be the case for $D < 2.25$, where the procedure does not yield a reliable result, suggesting that we are too far removed from the percolation threshold for the scaling relation to be valid.
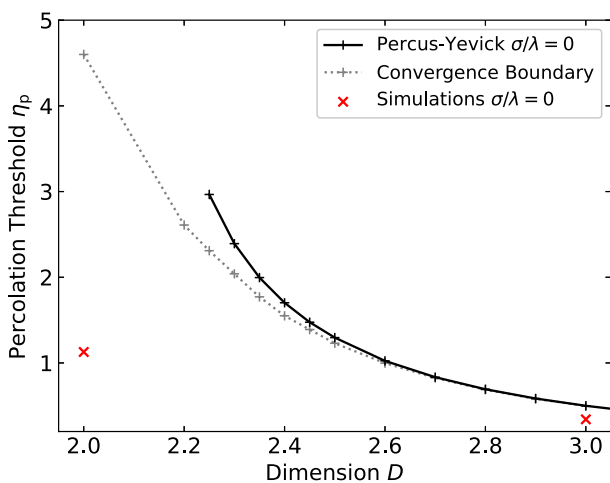

FIG. 6. The percolation threshold η_p as function of the spatial dimension D for ideal particles with $\sigma/\lambda = 0$. The percolation threshold is expressed as the number density scaled with the volume of a D-dimensional sphere of diameter λ. Our numerical solutions are shown in black. For $D < 3$ we include the convergence boundary of our numerical solver, i.e., the highest density for which our numerical solver remains stable and converges to a solution.
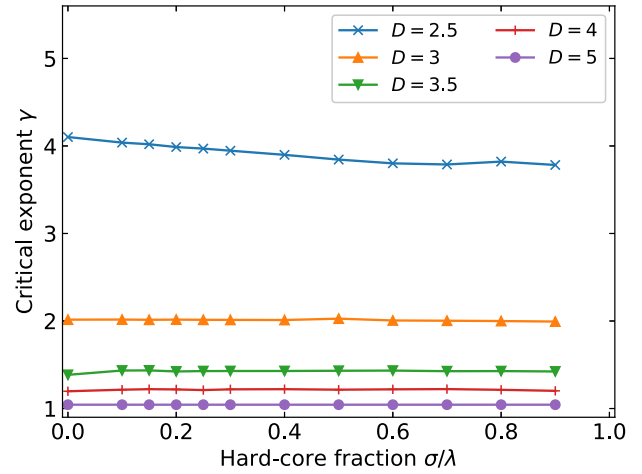

FIG. 7. The critical exponent γ within cPY theory as function of σ/λ for $D = 2.5$ (cross), $D = 3$ (triangle-up), $D = 3.5$ (triangle-down), $D = 4$ (plus), and $D = 5$ (dot).

APPENDIX B: UNIVERSALITY CLASS

The cherry-pit and ideal particle models are generally assumed to be part of the same universality class within percolation theory [23]. Focusing on the mean cluster size critical exponent γ only, analytical work shows that within cPY theory, the ideal and cherry-pit particles in $D = 3$ indeed both yield the same critical exponent [27,31]. We have numerically extended this analysis to $2.5 < D < 5$, the results of which we summarize in Fig. 7. For $D < 2.5$, we have not been able to accurately obtain the critical exponent for $\sigma/\lambda \neq 0$. The values that we find for the critical exponent for the case of small connectivity range $\sigma/\lambda > 0.9$ we do not include in the figure for all dimensions D. The reason is we find its value to suddenly drop considerably, contradicting known analytical results for $D = 3$ indicating that in this limit our predictions might not be reliable.

From Fig. 7, we conclude that the critical exponent is (nearly) independent of σ/λ, which strongly suggests that the ideal and cherry-pit particle models are part of the same universality class. The case for $D = 2.5$ might suggest that the critical exponent slightly decreases with σ/λ. We note, however, that this decrease also manifests itself for $D > 2.5$, albeit to a lesser extent. However, since the analytical solutions for the cherry-pit model in $D = 3$ have shown that the critical exponent is constant irrespective of σ/λ, we associate this with a (minor) error in our numerical solution.

APPENDIX C: ANALYTICAL SOLUTION

We are able to obtain the mean cluster size S for ideal particles in five dimensions within cPY theory, using the known connection between the isothermal compressibility for *hard particles* and the mean cluster size for *ideal particles* [51]. This result has, to our knowledge, not yet been reported in literature. Starting from the analytical expression for the compressibility derived in Ref. [52], we find the mean cluster

size in five dimensions to obey the expression

$$S(D=5) = \frac{9(1+\eta)^6}{f(\eta)(2-3\eta+\sqrt{f(\eta)})^2}, \qquad \text{(C1)}$$

with $f(\eta) = (1 - 18\eta + 6\eta^2)$. The smallest real root of this expression yields the percolation threshold and is given by

$\eta = \eta_{\mathrm{p}} = 3/2 - 5/6\sqrt{3}$. We obtain the critical exponent γ by expanding the mean cluster size S near the percolation threshold, the lowest order term of this expansion yields

$$S(\eta \to \eta_{\mathrm{p}}) = \frac{125(7\sqrt{3}-12)}{72(\eta-\eta_{\mathrm{p}})}, \qquad \text{(C2)}$$

from which we conclude that $\gamma = 1$ in five dimensions.

[1] M. Heinen, S. K. Schnyder, J. F. Brady, and H. Löwen, Phys. Rev. Lett. **115**, 097801 (2015).

[2] Y. Li, J. J.-Y. Suen, E. Prince, E. M. Larin, A. Klinkova, H. Thérien-Aubin, S. Zhu, B. Yang, A. S. Helmy, O. D. Lavrentovich, and E. Kumacheva, Nat. Commun. **7**, 12520 (2016).

[3] Q. Ji, R. Lefort, and D. Morineau, Chem. Phys. Lett. **478**, 161 (2009).

[4] W. G. Madden and E. D. Glandt, J. Stat. Phys. **51**, 537 (1988).

[5] J. A. Given and G. Stell, J. Chem. Phys. **97**, 4573 (1992).

[6] M. Schmidt, J. Phys.: Condens. Matter **17**, S3481 (2005).

[7] M. H. W. Chan, K. I. Blum, S. Q. Murphy, G. K. S. Wong, and J. D. Reppy, Phys. Rev. Lett. **61**, 1950 (1988).

[8] M. D. Dadmun and M. Muthukumar, J. Chem. Phys. **98**, 4850 (1993).

[9] D. W. Brown, P. E. Sokol, and S. N. Ehrlich, Phys. Rev. Lett. **81**, 1019 (1998).

[10] G. S. Iannacchione, G. P. Crawford, S. Žumer, J. W. Doane, and D. Finotello, Phys. Rev. Lett. **71**, 2595 (1993).

[11] A. V. Kityk, M. Wolff, K. Knorr, D. Morineau, R. Lefort, and P. Huber, Phys. Rev. Lett. **101**, 187801 (2008).

[12] E. C. Oğuz, M. Marechal, F. Ramiro-Manzano, I. Rodriguez, R. Messina, F. J. Meseguer, and H. Löwen, Phys. Rev. Lett. **109**, 218301 (2012).

[13] M. W. Maddox and K. E. Gubbins, J. Chem. Phys. **107**, 9659 (1997).

[14] L. D. Gelb, K. Gubbins, R. Radhakrishnan, and M. Sliwinska-Bartkowiak, Rep. Prog. Phys. **62**, 1573 (1999).

[15] C. Alba-Simionesco, B. Coasne, G. Dosseh, G. Dudziak, K. Gubbins, R. Radhakrishnan, and M. Sliwinska-Bartkowiak, J. Phys.: Condens. Matter **18**, R15 (2006).

[16] D. de las Heras, E. Velasco, and L. Mederos, Phys. Rev. Lett. **94**, 017801 (2005).

[17] Y. Gefen, B. B. Mandelbrot, and A. Aharony, Phys. Rev. Lett. **45**, 855 (1980); Y. Gefen, A. Aharony, and B. B. Mandelbrot, J. Phys. A: Math. Gen. **16**, 1267 (1983); Y. Gefen, A. Aharony, Y. Shapir, and B. B. Mandelbrot, *ibid.* **17**, 435 (1984); Y. Gefen, A. Aharony, and B. B. Mandelbrot, *ibid.* **17**, 1277 (1984).

[18] A. L. Windus and H. J. Jensen, Physica A **388**, 3107 (2009).

[19] V. Popa-Nita and S. Romano, Chem. Phys. **264**, 91 (2001).

[20] L. Radzihovsky and J. Toner, Phys. Rev. B **60**, 206 (1999).

[21] D. E. Feldman, Phys. Rev. Lett. **84**, 4886 (2000).

[22] M. Hvozd, T. Patsahan, and M. Holovko, J. Phys. Chem. B **122**, 5534 (2018).

[23] S. Torquato, *Random Heterogeneous Materials: Microstructure and Macroscopic Properties*, Interdisciplinary Applied Mathematics, Vol. 16 (Springer, New York, 2002).

[24] A. Coniglio, U. D. Angelis, and A. Forlani, J. Phys. A: Math. Gen. **10**, 1123 (1977).

[25] I. Balberg, J. Phys. D **42**, 064003 (2009).

[26] G. Ambrosetti, C. Grimaldi, I. Balberg, T. Maeder, A. Danani, and P. Ryser, Phys. Rev. B **81**, 155434 (2010).

[27] T. DeSimone, S. Demoulini, and R. M. Stratt, J. Chem. Phys. **85**, 391 (1986).

[28] J. P. Hansen and I. R. McDonald, *Theory of Simple Liquids: With Applications to Soft Matter*, 4th ed. (Academic Press, Oxford, 2013).

[29] E. Katzav, R. Berdichevsky, and M. Schwartz, Phys. Rev. E **99**, 012146 (2019).

[30] J. A. Barker and D. Henderson, Rev. Mod. Phys. **48**, 587 (1976).

[31] Y. C. Chiew and E. D. Glandt, J. Phys. A: Math. Gen. **16**, 2599 (1983).

[32] Moreover, barring series-expansion-type closures, as far as we are aware, all closures that predict a percolation threshold reasonably well are of the Percus-Yevick-type, in which the short-ranged restriction on $C^+(r)$ is modified [53]. It remains unclear how to correctly extend this to arbitrary dimensions without relying on *ad hoc* adjustable parameters.

[33] A. Drory, Phys. Rev. E **55**, 3878 (1997).

[34] C. D. Lorenz and R. M. Ziff, J. Chem. Phys. **114**, 3659 (2001).

[35] S. Torquato and Y. Jiao, J. Chem. Phys. **137**, 074106 (2012).

[36] I. Balberg, C. H. Anderson, S. Alexander, and N. Wagner, Phys. Rev. B **30**, 3933 (1984).

[37] S. Torquato, J. Chem. Phys. **136**, 054106 (2012).

[38] C. Grimaldi, Phys. Rev. E **92**, 012126 (2015).

[39] S. B. Lee and S. Torquato, Phys. Rev. A **41**, 5338 (1990).

[40] M. A. Miller, J. Chem. Phys. **131**, 066101 (2009).

[41] A. L. R. Bug, S. A. Safran, G. S. Grest, and I. Webman, Phys. Rev. Lett. **55**, 1896 (1985).

[42] C. Grimaldi, J. Chem. Phys. **147**, 074502 (2017).

[43] R. J. Baxter, *Exactly Solved Models in Statistical Mechanics* (Academic Press, London, 1982).

[44] J. Adler, Y. Meir, A. Aharony, and A. B. Harris, Phys. Rev. B **41**, 9183 (1990).

[45] F. Coupette, R. de Bruijn, P. Bult, S. Finner, M. A. Miller, P. van der Schoot, and T. Schilling, Phys. Rev. E **103**, 042115 (2021).

[46] F. Coupette, A. Härtel, and T. Schilling, Phys. Rev. E **101**, 062126 (2020).

[47] J. D. Talman, J. Comput. Phys. **29**, 35 (1978).

[48] A. J. S. Hamilton, Mon. Not. R. Astron. Soc. **312**, 257 (2000).

[49] M. Heinen, E. Allahyarov, and H. Löwen, J. Comput. Chem. **35**, 275 (2014).

[50] A. Kovalenko, S. Ten-no, and F. Hirata, J. Comput. Chem. **20**, 928 (1999).

[51] G. Stell, J. Phys. A: Math. Gen. **17**, L855 (1984).

[52] E. Leutheusser, Physica A **127**, 667 (1984).

[53] J. A. Given and G. Stell, in *On Clusters and Clustering*, Random Materials and Processes, edited by P. J. Reynolds (North-Holland, Amsterdam, 1993), pp. 357–372.